Chapter 1

Background of Graphene and its applications

1.1. Introduction

Graphene, a unique two-dimensional (2D) material, has been continuously tempting to the scientific research community owing to its exceptional thermal, mechanical, electrical and optical properties [1]-[4]. It was extracted as a planar material using adhesive tape in 2004 from the research lab at University of Manchester [1]. Graphene is a two-dimensional (2D) allotrope of carbon [2]-[3]. Carbon has different physical forms *viz.*, fullerene (0D), carbon nanotubes (1D), graphite (3D), diamond (3D), etc. [4]. The chemical composition and structural details resemble graphene as a one atom-thick slice of the graphite (3D) crystal with hexagonal lattice having an exceptionally larger value of tensile

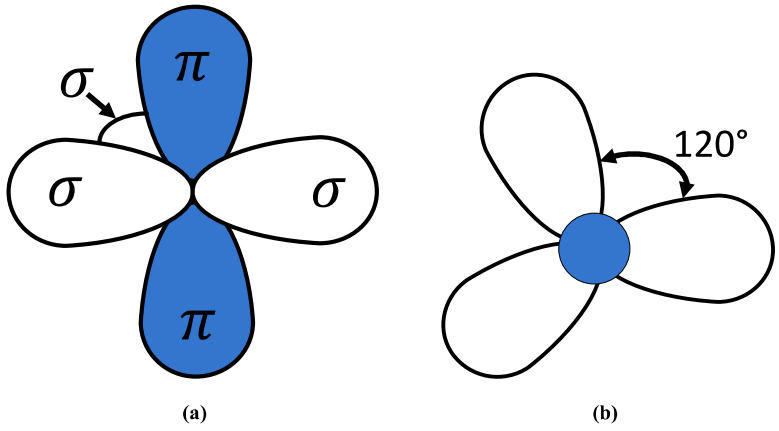

Fig. 1.1. Schematic representation of formation of covalent bonds in graphene surface.

strength of 130 gigapascals [5]. One single atom of carbon has four electrons in its outermost orbital during the covalent bonding process. The electrons distributed along the horizontal

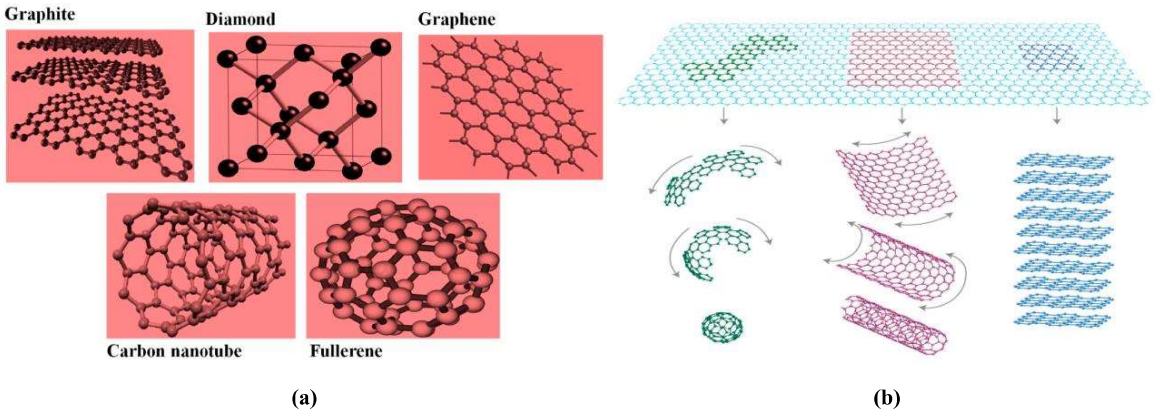

Fig. 1.2. Schematic representation of the (a). different physical forms of carbon and (b). formation of the allotropes [4].

plane form sigma bond whereas the π-electrons placed along the vertical plane are delocalized and energetically stable on the 2D graphene surface as depicted in Fig. 1.1 [4]. This plays a key role in achieving high-rise in mobility of the electrons distributed along the 2D graphene plane resulting in a high value of electrical surface conductivity (σ). Pristine graphene, an original, pure and unoxidized form of graphene, is a zero-bandgap semi-metal and preferred in the field of nanotechnology research area as the conduction band and valance band of the honeycomb graphene structure intersect to several dirac points [5]. Graphene has the highest ratio of edge atoms among all the physical forms of carbon as shown in Fig. 1.2; thereby leading to maximum number of times more chemical reactivation than thicker sheets [6]-[7]. Graphene is very much suitable for optical applications as it is having an inherent-optical absorption; it can absorb electromagnetic (EM) wave at any spectral region together with the terahertz (THz) domain.

Terahertz-gap (0.1 THz-10 THz), spanning in between two well-established spectral domains, *viz.*, the photonics domain on the higher end and the electronics domain on the lower end of the frequency spectrum, is promising for the limitless futuristic applications towards industrial

and manufacturing purposes as EM wave can be used optically, electronically or both optically and electronically in terms of generation, detection or manipulation of the wave. THz is getting

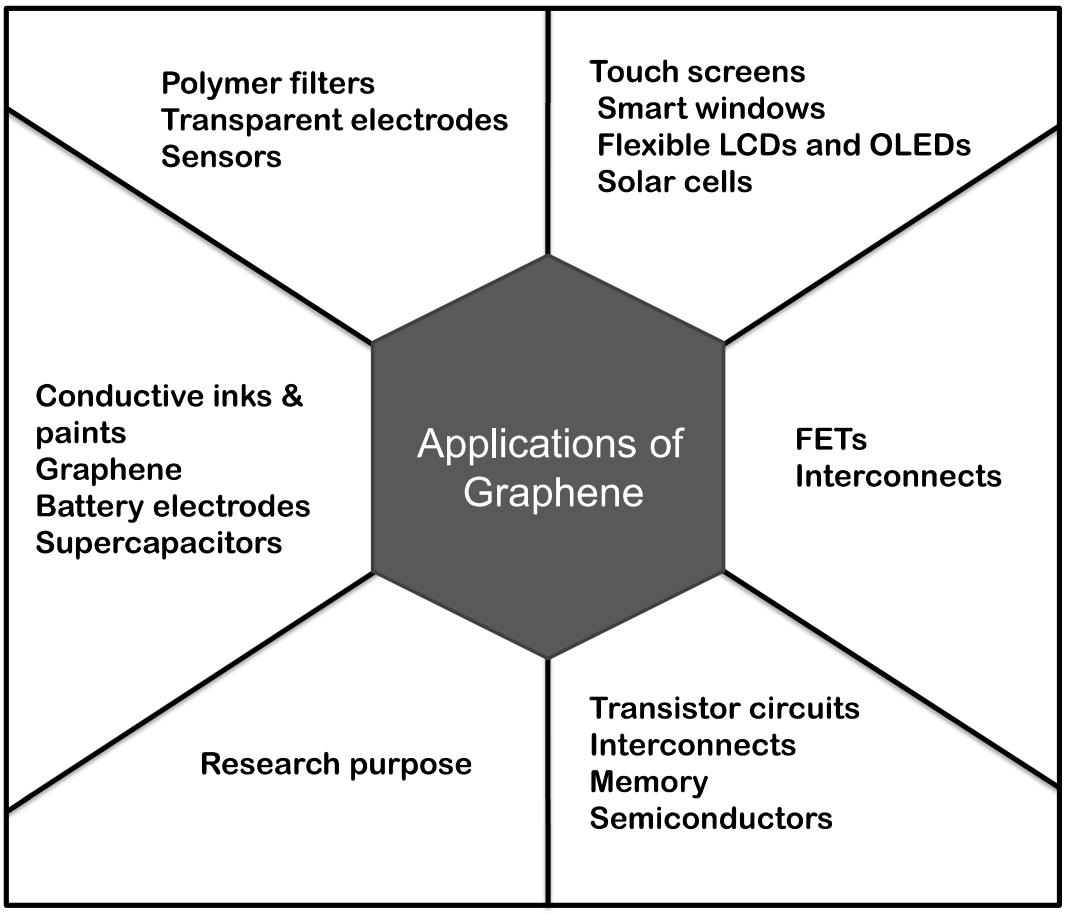

Fig. 1.3. Current applications of graphene and graphene derivatives. Reproduced from [4].

attention of the scientific research community because of its distinctive spectral characteristics [8]. THz emission and absorption spectrum of molecules are being utilized for the space exploration [9]. THz radiation has been used in security and medical applications [10] for the imaging of the human body as it is non-ionizing in nature; thereby producing least health issues than X-ray radiation. The modern wireless communication systems have also been improved with increased channel capacities for wideband short-range communication [11].

THz field needs more research on the support investigations of the material properties. A few three-dimensional (3D) materials have been properly characterized for THz spectral region,

viz., silicon dioxide [12] or gold [13], etc. Recently, some two-dimensional materials, *viz.*, borophene [14], silicene [15], phosphorene [16] have also shown interesting electronic and optical properties to be potential candidate for EM applications. Currently, graphene has a number of applications in different fields as shown in Fig. 1.3 [4], [17].

1.2. Mathematical Basis of Graphene

Atomically-thin, monolayer graphene can be assumed to be an infinitesimally thin surface with the bandgap energy tending to zero. The surface conductivity of graphene plays the key role to determine the electromagnetic characteristics of the graphene-based devices. It can be formulated by some specific equations provided by Kubo [18] as discussed in equation (1.1)-(1.4).

$$\sigma_g(\omega, E_f, \Gamma, T) = \sigma_{inter} + \sigma_{intra} \tag{1.1}$$

$$[\sigma_g]_{intra} = \frac{2k_bTe^2}{\pi\hbar^2} ln\left(2\, cosh\frac{E_f}{2k_bT}\right)\frac{i}{(\omega+i\Gamma)} \tag{1.2}$$

$$[\sigma_g]_{inter} = \frac{e^2}{4\hbar}\left[H\left(\frac{\omega}{2}\right) + i\frac{4\omega}{\pi}\int_0^\infty \frac{H(\Omega)-H\left(\frac{\omega}{2}\right)}{\omega^2-4\Omega^2}d\Omega\right] \tag{1.3}$$

$$H(\Omega) = sinh\left(\frac{\hbar\Omega}{k_bT}\right)/\left[cosh\left(\frac{\hbar\Omega}{k_bT}\right) + cosh\left(\frac{E_f}{k_bT}\right)\right] \tag{1.4}$$

Here, graphene exhibits uncommon surface conductivity, which is essential for the manipulation of the EM wave at the mid-infrared (MIR) spectrum. σ_g is a complex function having two constituents, *viz.*, intraband conductivity and interband conductivity, as provided in equation (1.2) and (1.3), respectively. The chemical potential of graphene (μ) can be influenced by the external parameters, *viz.*, chemical doping, mechanical straining or biasing of the graphene layer on a proposed device, *i.e.*, the device under test (DUT). In this regard, k_B stands for the Boltzmann's constant, e points out to the charge of an electron, E_f describes the Fermi energy of graphene, ω is termed as the angular frequency of the photon, T is taken to be 300 K, operating room temperature, Γ, which is inversely changing with the relaxation time, τ, is described as the scattering rate of the Dirac electrons, $\hbar$ is referred to the reduced Plank's constant, and the Fermi dirac distribution function has been represented as $f_d(\varepsilon) = \left(e^{\frac{(\varepsilon-\mu)}{k_BT}} + 1\right)^{-1}$; here, ε is equal to the associated energy. The dispersive transfer function has been represented in equation (1.4) [18].

The intraband conductivity has a dominant effect over the interband part when the Fermi level is larger than half of the energy of a photon ($\hbar\omega < 2E_f$). Under this condition, the latter has a negligible impact on the total surface conductivity owing to Pauli blocking [19]. The external electrical biasing effect on Fermi level of graphene can be formulated as provided in equation (1.5). The Drude model guides that

$$E_f = \hbar v_f \sqrt{\frac{\pi \varepsilon_p \varepsilon_o \mu}{et^2}} \qquad (1.5)$$

the surface conductivity of graphene (σ_g) is directly proportional to the Fermi level (E_f) till infrared region, as verified from equation (1.6) [20]. The relative permittivity $\varepsilon(\omega)$ is directly proportional to σ_g, where the thickness of the 2D graphene layer is noted by t_g as encountered in equation (1.7). The single layer graphene is normally contemplated as an ultrathin film with the thickness of 1 nm [21]-[23].

$$\sigma_g = \frac{e^2 E_f}{\pi\hbar^2} \cdot \frac{i}{\omega + i\tau^{-1}} \qquad (1.6)$$

$$\varepsilon(\omega) = 1 + i\frac{\sigma_g(\omega)}{t_g \varepsilon_o(\omega)} \qquad (1.7)$$

$$\sigma_{xx} = \sigma_{yy} = \sigma_g(\mu(E_o)) \qquad (1.8)$$

The surface conductivity of graphene is generally a scalar value under the influence of the DC electrostatic bias (E_o) and in absence of the DC magnetostatic one, as shown in equation (1.8) [24].

$$\sigma_{xx} = \sigma_{yy} = \sigma_g(\mu(E_o)) \qquad (1.8)$$

This idea derives a simple linear connection between σ_g and μ which is further a function of the external electric field (E_o). The DC gate voltage can be calculated in a systematic way as $V_g = E_o d$, d being the substrate thickness. Thus, it is evident that μ is a direct function of E_o. The formulation of the surface charge density (n_s) of the 2D graphene surface can be expressed in equation (1.9), where C_{ox} is the gate

$$C_{ox}E_o = en_s \qquad (1.9)$$

capacitance, v_f points out to the Fermi velocity of the electrons distributed along the 2D graphene surface; which is further measured as 10^6 m/s and E_o indicates the applied DC electrostatic bias. The quantum capacitance is least significant due to the large thickness of the dielectric substrate [25]. The solution of E_o has been derived under the condition of undoped and ungated case, *i.e.,* $\mu = n_s = 0$; the

$$n_s = \frac{2}{\pi\hbar^2 {v_f}^2}\int_0^\infty \varepsilon[f_d(\varepsilon-\mu) - f_d(\varepsilon+\mu)]\,d\varepsilon \qquad (1.10)$$

equation (1.10) has been deduced from this concept where ε_b is the effective permittivity of the substrate in the expression $D_n = \varepsilon_b E_o = en_s/2$. $D_n$is the normalized part of the displacement vector quantity

$$\frac{2\varepsilon_b E_o}{e} = \frac{2}{\pi\hbar^2 {v_f}^2}\int_0^\infty \varepsilon[f_d(\varepsilon-\mu) - f_d(\varepsilon+\mu)]\,d\varepsilon \qquad (1.11)$$

distributed on each side of a charged sheet within a homogeneous dielectric substrate having an effective permittivity value of ε_b [26]. The highest value of the chemical potential μ_{max} can be realized by following the equation (1.12); further revealed in equations (1.13) and (1.14), where the breakdown voltage of the dielectric substrate, E_{bd} plays an important role. The calculated measure of E_{bd} is ~ 1.5 V/nm for silicon dioxide (SiO_2) substrate with an effective permittivity value of ε_r= 3.9 [26]-[27].

$$E_o = \frac{e}{\pi\varepsilon_b b\hbar^2 {v_f}^2}\int_0^\infty \varepsilon[f_d(\varepsilon-\mu) - f_d(\varepsilon+\mu)]\,d\varepsilon \qquad (1.12)$$

$$E_o \simeq \frac{e}{\varepsilon_o\varepsilon_r}\frac{1}{\pi}\left[\frac{\mu}{\hbar v_f}\right]^2 \qquad (1.13)$$

$$\mu_{max} = hv_f\sqrt{\frac{\pi\varepsilon_o\varepsilon_r E_{bd}}{e}} \qquad (1.14)$$

Graphene had been historically first associated with the electronics applications, *viz.*, in a transistor with an operating speed doubled *w.r.t.* its silicon counterpart by IBM in 2011 [28]. After that, wafer-scale based graphene-made electronic devices have been surfaced [29]. The flexible electronics industry can find a way to achieve high performance in the transistors by the synthesis of graphene spanned over a large area [30]. Hybrid configurations of the graphene-based transistors have got the attention of the scientific community lately, owing to the least base transit time induced by the single-atom thick graphene layer [31]. In the same way, graphene-based RF field-effect transistors (FETs), 2D-metal-

oxide-semiconductor capacitor, other 2D heterostructures, and frequency multipliers have also been surfaced to date [32]-[35]. However, the research in making graphene-based FETs is not so successful owing to the bandgap issue.

1.3 Properties of Graphene

1.3.1 Linear Properties of Graphene

Fermi energy of the electrons on the graphene surface plays a crucial role in the optical absorption of the electromagnetic wave. The optical absorption under the undoped condition at 0 K temperature is not dependent on the frequency and this fact can be verified from the fine structure constant, as discussed in [36], and it can be calculated by the equation $A = \pi\alpha \approx 2.3\%$, where $\alpha = e^2/\hbar = 1/137$. Two different types of losses have been occurred depending on the carrier concentration and basically, they are generated from the two separate mechanisms: intraband and interband losses. The interband transition occurs when one electron from the valance band is excited by the photon and it reaches the conduction band if the energy of the photon is more than $2E_F$ ($\hbar\omega > 2E_F$). In this case, in infrared and visible region (short wavelengths), the optical conductivity of graphene is almost independent of the Fermi energy [37]. Contrarily, graphene plasmons can transfer their energy to the electrons scattering from the charged impurities. This particular transition process places the electron in the conduction band, and it is called as an intraband transition ($\hbar\omega \leq 2E_F$). The graphene layer behaves like a conductive sheet in THz region (long wavelengths) and the optical conductivity of graphene will follow its electrical conductivity. The optical conductivity of graphene (2D surface) can be expressed by Kubo's equation [18], as stated earlier. The minimum optical conductivity can be derived by assuming the Fermi energy (E_F) and temperature (T) are equal to zero and it can be found from the expression: $\sigma_0 = e^2/4\,\hbar$. Therefore, the optical characteristics of a truly 2D material can be completely described by the equation, $J = \sigma E$, where J refers to the surface conductivity of graphene and E points out to the in-plane electric field component. Under the exposure of the incident EM field, interband and intraband transitions have been induced on the graphene surface which can be experienced in Fig. 1.4. These two distinct transitions are the origin of optical conductivity, as discussed in [18]. It can also be established that the intraband contribution to the surface

conductivity of graphene dominates over the interband counterpart in the THz (long wavelengths) region. The distinctive characteristics of ballistic transport and high electron mobility (more than 20000 cm^2/Vs) may be responsible for the purely imaginary conductivity of graphene within the above-said region [26].

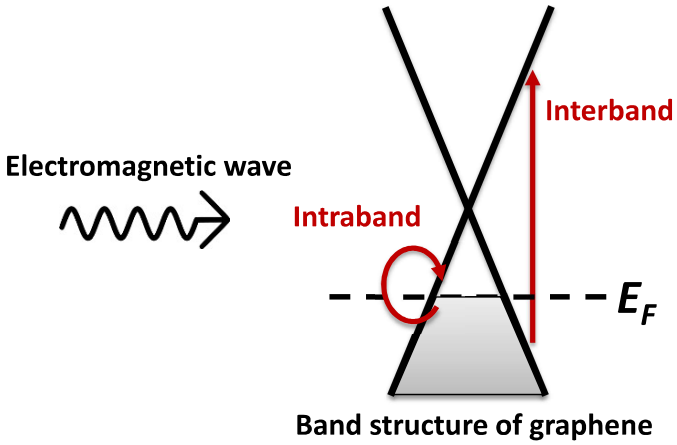

Fig. 1.4. Interband and intraband transitions induced by wave in doped graphene.

The real and imaginary components of the surface conductivity of graphene for both the interband and intraband transitions have been described in terms of the universal optical conductivity, as functions of the photon energy, described in [38]. The temperature has been considered as the room temperature. i.e., 300 K. It can be well established that the intraband conductivity (σ_{intra}) dominates over the low-frequency region while the interband conductivity (σ_{inter}) rules in high-frequency range, which further shows Pauli blocking, when $\hbar\omega \geq 2E_f$ and move toward the universal conductivity (σ_0) at high spectral region. The specific format for the equation (1.1) suggests that σ_{intra} primarily follows Drude equation. More specifically one can determine that the surface conductivity of graphene can be tuned with the variation of the Fermi level (E_f). This dynamic reconstruction in graphene's chemical properties can be utilized for tailoring an individual graphene-based device for varieties of application purposes operating over a wide span of optical frequencies from THz to visible region [39]. Electro-optic modulation can also occur due to the application of the external gate signals [40]. Surface carrier transfer has also shown a way to alter the Fermi level of graphene up to 0.8 eV enabling the coupling of the graphene plasmons in the near-infrared

spectrum [41]. A recent study [42] has confirmed further up to 1 eV to improve the above-said coupling of the graphene plasmons.

In this thesis, we have designed and analyzed several graphene-based devices for the THz applications, where the interband transitions have the least effect on the total surface conductivity of graphene, as discussed previously. Therefore, the surface conductivity of graphene has been modelled following Drude mathematics [43], as shown in equation (1.15).

$$\sigma_g = -\frac{iD}{\pi(\omega - i\tau^{-1})} \tag{1.15}$$

Here, $D = e^2 E_f/\hbar^2$ and τ represents the electron relaxation time which is further responsible for the optical loss.

1.3.2 Non-linear Properties of Graphene

Graphene shows its nonlinearity property at very high intensities of light generated by lasers. Two-dimensional (2D) materials having great photophysical characteristics and optical nonlinearities are the suitable options for the applications within the THz frequency region [14]-[17]. Graphene exhibits extraordinary optoelectronic properties and optical nonlinearities having very high-speed response times over a wide frequency range [4]. Lately, various optical characteristics of graphene have been rigorously studied and experimented, *viz.*, mixing of frequencies, optical rectification, harmonic generation and photon drag effect [44]-[48], leading to the futuristic applications, such as, THz transistors, optical power limiting, fast optical communication and all-optical switches [49]-[53].

The nonlinearity of graphene can be theoretically examined under the influence of an external electric field to the graphene surface and the nonlinear dynamics can be observed in the form of induced electric currents. It has been surfaced that graphene can have very strong nonlinearities at THz and microwave frequency regions, and its resulting responses can be checked with the low magnitudes of the fields (10^3 V/cm) [45], [51], [47], generated from the band structure of graphene. The nonlinearity response of graphene sourced from the relation between the carrier velocity is not proportional to the momentum under an oscillating EM field; unlike the parabolic band semiconductors.

1.3.3. Metals at optical frequencies

In this section, the behavior of metals at high frequencies has been discussed. Generally, metasurface structures bear metallic components within a meta-atom. In this context, Drude free electron model offers a more practical method of modeling metals than the conventional conductor model approach. This is because of the fact that the inertial effect owing to the finite value of the of the electron mass plays an important role. The valance electrons are loosely bound to the nucleus; thereby following random motion inside the metal. Under the exposure of the incident EM wave the behavior of the metals is dependent on the inclusive movement of the free electrons (denoted as 'N') which moves against the positive core nucleus. Drude model is a classical approach that that which assumes material to be a free-electron gas spreading around the relatively heavy positive ions. The whole system of the negatively-charged free-electron gas and the positive nucleus core has been reduced to a neutral medium called plasmas. Drude model is dependent on two important aspects, i.e., (a). The electrons follow a locus of a straight line in between collisions when the EM wave is not present. Therefore, the interactions between electron-electron or electron-ion are ignored.

(b). The time duration between the two collisions (τ) is independent of the velocity and position of the electrons. The probability of collision per unit time is called collision frequency or scattering rate ($\Gamma = {}^{1}/_{\tau}$).

The electrons on the metal surface will get accelerated under the exposure of the time-harmonic incident electromagnetic field ($E_0 e^{-j\omega t}$) given by equation (1.17).

$$m\frac{d^2x(t)}{dt^2} = qE \qquad (1.17)$$

Here, m and e stand for the effective mass and the charge of the free electrons. It signifies that the electrons undergo acceleration while an electric field will be applied across them. In practice, electrons undergo collisions with each other during the movement and a resistive force inhibiting electron motion has been included to form the expression in (1.18).

$$m\frac{d^2x(t)}{dt^2} + m\gamma\frac{dx(t)}{dt} = qE \qquad (1.18)$$

γ stands for the damping constant. The double derivative term of the above expression represents the inertial force and the single derivative term points out the loss evolved owing to the collision of electrons. The solution to the above expression can be reduced to the following:

$$x(t) = -\frac{q}{m}\frac{1}{\omega(\omega+i\gamma)}e^{(-j\omega t)} \qquad (1.19)$$

The polarization density can be evaluated as $P = Nex(t)$, where N stands for the density of the free electrons, $x(t)$ is the measure of change of the positions of the electrons from their initial state. The applied electric field and the electric displacement are related as:

$$D = \varepsilon_0 E + P \qquad (1.20)$$

$$\text{Here, } P = -\frac{Ne^2}{m}\frac{1}{\omega(\omega+i\gamma)}$$

The above equation can be reduced to the following form after incorporating the value of P in terms of the relative permittivity ($\varepsilon(\omega)$) of the metallic material provided below.

$$\varepsilon(\omega) = 1 - \frac{[\omega_p]^2}{\omega(\omega+i\gamma)} \qquad (1.21)$$

In this context, ω_p represents the plasma frequency at which the electrons gas oscillates, estimated as:

$$\omega_p = \sqrt{\frac{Ne^2}{me_0}} \qquad (1.22)$$

Table 1.1. Plasma frequency for metals

Noble Metals	**Plasma frequency (f_p) (THz)**
Gold (Au)	2176 THz
Silver (Ag)	2186 THz
Aluminium (Al)	3570 THz

Table 1.1 describing the values of the plasma frequencies of some noble metals has been included in this section.

1.3.4 Surface Plasmons in Graphene

In electromagnetics, a surface wave is usually formed at the interfaces between two different materials with different refractive indices employing two half-spaces. The surface wave concept will not be applicable if the two materials are identical in terms of their refractive index profiles. This fact also validates that surface waves cannot always be generated comprising any combination of materials. Surface plasmon polaritons (SPPs) are an essential property in plasmonics, and is formed due to the coupling between the electric fields and oscillations of the electron plasma in the material [54]. The confinement of the wave in terms of the fields at the dielectric interfaces occurs due to dissimilar refractive indices profiles while EM wave is incident on the periodic metallic metasurface structures [55]. A pictorial illustration of the different configurations of the single-layer dielectric-metal interface and multilayer dielectric-metal interfaces have been depicted in Fig. 1.5(a) and Fig. 1.5(b), respectively. The term q_{spp} embedded in the figure stands for the wave vector of the SPP mode. An elaborate explanation

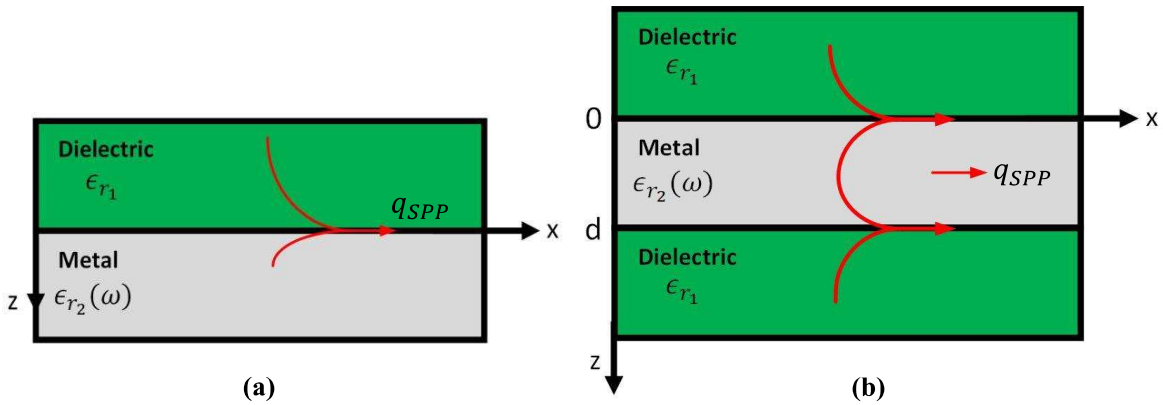

Figure 1.5. Schematic representation of the formation of SPP at (a) a dielectric-metal interface and (b) interfaces between dielectric-metal-dielectric structures.

suggests that the formation of SPPs has been described in two different configurations, *viz.*, a dielectric-metal interface and other interfaces between dielectric-metal-dielectric materials as

conferred from Fig. 1.5. In case of Fig. 1.5(a), two media are taken to be semi-infinite and isotropic with the dielectric material engaging half-space ($z < 0$). The dielectric material can be interpreted in terms of a positive real dielectric constant ϵ_{r1}, and the metal can be expressed by Drude model [56], as shown in equation (1.23):

$$\epsilon_{r2}(\omega) = 1 - \frac{{\omega_p}^2}{\omega^2 + i\omega\gamma} \qquad (1.23)$$

In equation (1.23), where ${\omega_p}^2 = \frac{e^2 n_e}{m_e \epsilon_0}$ is the square of the plasma frequency of the electron gas; Γ stands for the scattering rate of the electrons. For the metal, $Re(\epsilon_{r2}(\omega))$ is always negative. This condition should be satisfied to support the longitudinal waves that are firmly concentrated to the interface between the different media, as discussed in Fig. 1.5. This type of

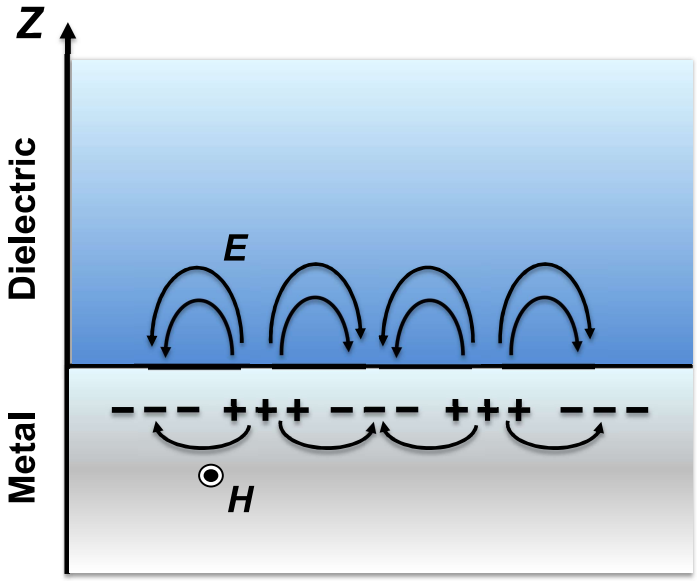

Figure 1.6. Schematic representation of the formation of SPP at the dielectric-metal interface.

surface waves are mentioned as SPP modes. A tri-layer heterostructure has been shown in Fig. 1.5(b). Usually, this set-up follows two different combinations, dielectric-metal-dielectric (DMD) or metal-dielectric-metal (MDM), in which SPP is formed at each of the dielectric-metal interfaces and metal-dielectric junction. The communication between the EM fields of the SPP modes of the two opposite junctions is feasible only when the thickness of the metal layer is negligibly small, known as hybridized mode. A representation of the hybridized mode

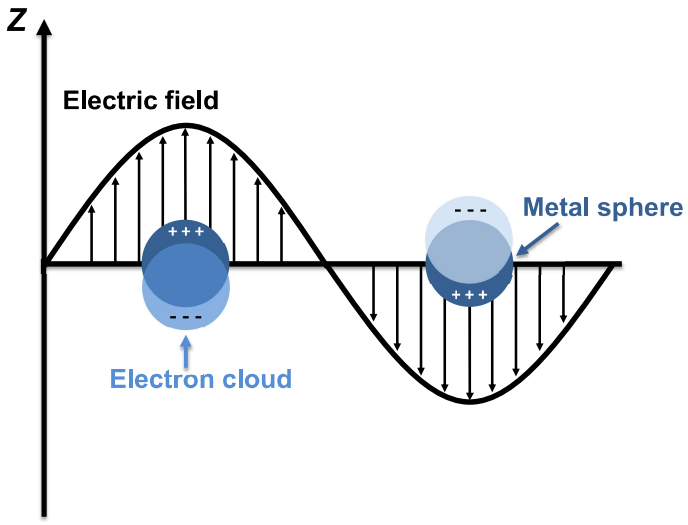

Figure 1.7. Schematic representation of the formation of LSPR around the metallic nanoparticles smaller than the incident wavelength.

is shown in Fig. 1.5(b) in red color. If the metallic region is replaced with the 2D graphene surface, the dispersion relation for the graphene surface plasmons (GSPs) can be explained by equation (1.24) as provided in [56].

$$\frac{\epsilon_{r1}}{k_1(q,\ \omega)} + \frac{\epsilon_{r2}}{k_2(q,\ \omega)} + i\frac{\sigma(\omega)}{\omega\epsilon_0} = 0 \qquad (1.24)$$

The annotations carry their usual meanings where $\sigma(\omega)$ is the dispersive surface conductivity of graphene, the SPP wave number function is denoted by k_j, which is a function of two variables, *viz.*, q and frequency (ω). The solution of the above-said equation (1.24) are real values only when the imaginary portion of $\sigma(\omega)$ is positive and the real component of $\sigma(\omega)$ is of zero value. The solution of the same equation (1.24) will reduce to a complex one when the real part of $\sigma(\omega)$ is finite.

Plasmonic waves can be generated along the metal surface, with the movement of the coupled photon energy induced by the collective motion of the free electrons as illustrated in Fig. 1.6 [60]. Graphene surface plasmons (GSPs) excitation is a method to efficiently enhance the nonlinear behavior of graphene. Previously, prism coupling configurations or grating

configurations have been used for the excitation of the GSPs. Localized surface plasmons (LSPRs) can be also generated independently on the periodic graphene structures using the concept shown in Fig. 1.7. Hence, graphene can be employed as an essential part of a device to offer field confinement or field enhancement by exploiting its plasmonic characteristics [61]-[62]. In recent times, GSP have been noticed in many graphene-based structural configurations, *viz.*, graphene surface with nano-slits, graphene ribbons, and graphene disks, etc [63]-[66]. GSPs have a unique feature called 'tunability', unlike the conventional metals. The behavior of the GSPs is dependent on the carrier concentration and can be dynamically controlled by doping chemically or under the effect of the external electric field [65], [67].

The plasmonic characteristics of graphene can be explained by using the concept of the semi-classical model. In three-dimensional (3D) devices, plasmas can be compatible with both the longitudinal and transverse EM modes. But in case of 2D electron gases, only the transverse magnetic mode (TM mode) is present under some specific experimental set-up. The TM plasmon mode for the suspended graphene surface and its dispersion relation can be expressed in equation (1.25) [68].

$$1 + \frac{2\pi i\sigma(\omega)\sqrt{k^2-\omega^2/c^2}}{\omega} = 0 \qquad (1.25)$$

Here, k denotes the wavenumber of the plasmonic mode. It also has a role to play as the local dynamic conductivity of 2D electron gas working as a function of ω. The TM mode comes into play when the imaginary component of the conductivity is positive, as can be concluded from equation 1.25. Transverse electric (TE) mode can be present in graphene and can propagate along the graphene layer having almost an equal velocity of light, c [69]. Graphene shows a weak damping effect due to the TE mode and offers tunable frequency response over a wide spectral span ranging from radio waves to the infrared [69]. Similarly, the dispersion relation for TE mode can be derived from the following expression provided in equation (1.26).

$$1 - \frac{2\pi i\sigma(\omega)}{c^2\sqrt{k^2-\omega^2/c^2}} = 0 \qquad (1.26)$$

One can determine from the above equation that the TE mode can also exist in graphene if and only if the imaginary component of the surface conductivity carries a negative value. Hence, we can conclude that the sign of imaginary part of $\sigma(\omega)$ determines the supporting mode.

$$k = \frac{\omega}{c}\sqrt{1 - \left[\frac{2\varepsilon_d\varepsilon_0 c}{\sigma(\omega)}\right]^2} \qquad (1.27)$$

Our primary focus in this thesis will be the futuristic electromagnetic applications in the THz frequency region only. Therefore, we have considered only the intraband conductivity for simplicity as interband conductivity has negligible impact within the above-said frequency range. The electronic susceptibility of graphene can be calculated as:

$$\chi_g = \frac{i\sigma_g k}{\varepsilon_0\omega} = -\frac{e^2E_f k}{\varepsilon_0\pi\hbar^2\omega^2} \qquad (1.28)$$

By incorporating the Drude model into the bulk plasma frequency, we can obtain

$$\omega = \sqrt{\frac{e^2E_f k}{\varepsilon_0\pi\hbar^2}} \qquad (1.29)$$

This conclusion has been made with the help of the semi-classical model which is valid under the condition $k \ll k_f$ [70]. Another form of the dispersion relation of the graphene plasmons can be found in the random phase approximation (RPA) technique [70]-[72]. The equation (1.29) discloses some important information about 2D Dirac plasmons, i.e., the plasma frequency of graphene changes according to the following expression:

$$E_f = h v_f\sqrt{\pi N} \qquad (1.30)$$

Thus, it can be concluded that the plasma frequency of the graphene plasmon changes with the Fermi energy by a direct proportional term $N^{1/4}$. Additionally, we can infer from equation (1.30) that the plasma frequency of graphene bears Plank's constant in place of the electron effective mass signifying the Dirac nature of the graphene plasmons.

1.4. Metasurface, Graphene-based Metasurface: Subsequent Developments

1.4.1 Metamaterials and Metasurfaces

The EM behavior of a homogeneous material in nature can be defined by its molecular composition. The materials are mainly explained by the constitutive parameters, *viz.*, electric

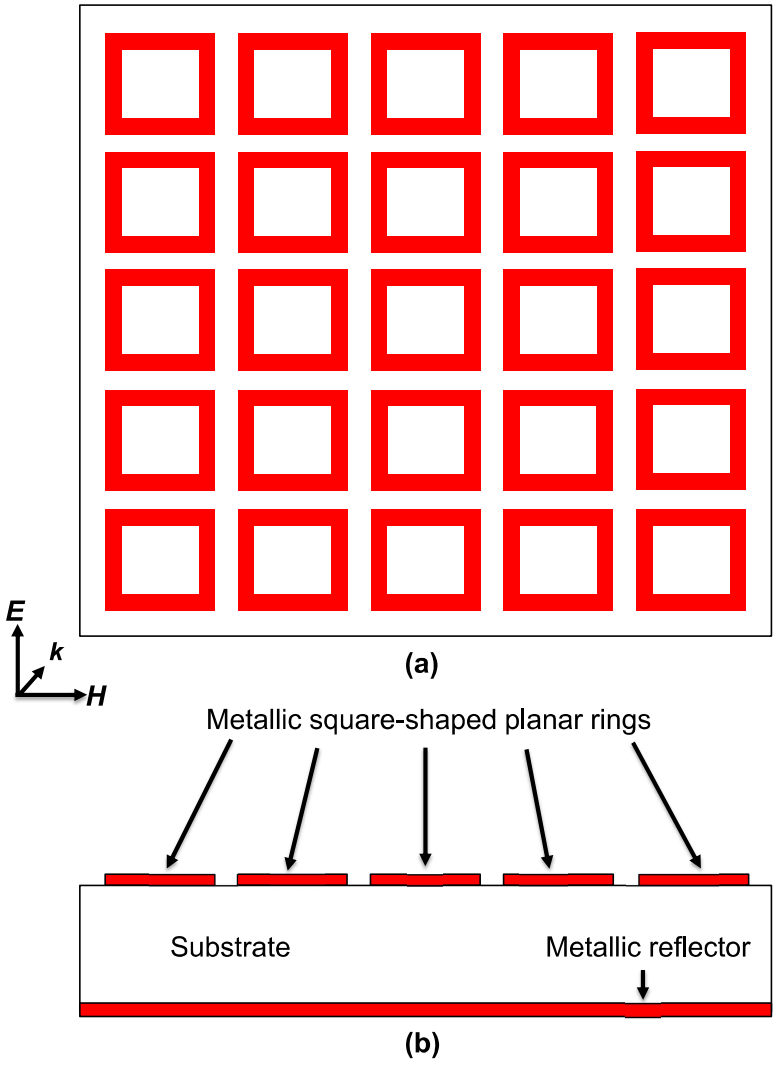

Fig. 1.8. Schematic representation of metasurface structures.

permittivity (ε) and magnetic permeability (μ) as the macroscopic forms of the electric and magnetic fields of an EM wave propagating through the material are acknowledged by the average of their microscopic forms of the fields [73]. Lately, the concept of 'metamaterial' was brought into the picture as a new type of artificial materials. The term 'meta' comes from the

Greek word '$\mu\varepsilon\tau\alpha$'; the meaning of this particular word is 'beyond'. Hence, metamaterials can be defined as materials having properties which are not available in nature unlike conventional materials [74]-[80]. In a similar way, a metamaterial can be designed to have a sub-wavelength thickness and a compact periodicity; thereby easily mountable to any circuit components by reducing the bulkiness of the whole electromagnetic system. This modern definition of the metamaterial is called 'metasurface', a two-dimensional (2D) counterpart of the former one. A simple schematic of the metasurface has been presented in Fig. 1.8. Usually, metasurfaces are being used in large numbers to manipulate the EM wave in the spectral domain. An excessive number of

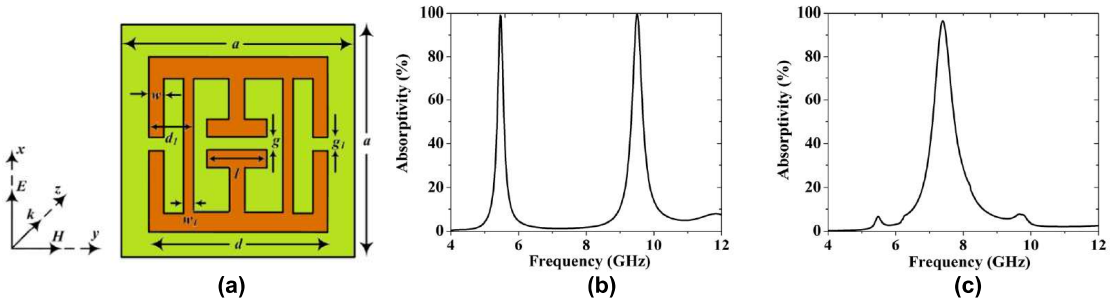

Figure 1.9. (a). Metallic metasurface structure for electromagnetic wave absorption and (b). dual-band absorptivity response under normal incidence and (c). single band absorptivity response under 90° polarization angle [81].

essential and useful applications of metasurfaces can be found in several fields, *viz.*, perfect absorbers, nanoantenna devices, cloaking and diffraction imaging etc. [74], [81]-[87]. Most of the proposed metasurface-based structures use the plasmonic behavior of their metallic components or meta-atoms and they show resonant responses. Plasmonic materials exhibit intense interaction with light by means of plasmonic resonances. Owing to the external electric field originating from the intense interaction, the electrons within the plasmonic material can be moved from their steady-state conditions. Therefore, a phase shift response can be produced at the interface between the metallic structure and the substrate material within a meta-atom. The metasurfaces assure a very useful stage to achieve light focusing, polarization conversion,

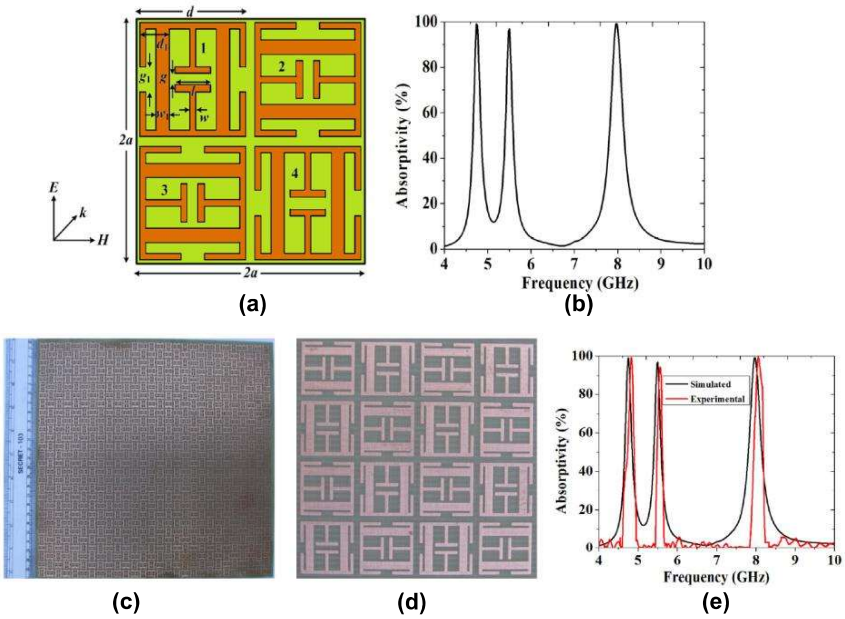

Figure 1.10. (a, b). Metallic metasurface structure for triple-band electromagnetic wave absorption and (c, d) fabricated prototype and (e). comparison of the simulated and measurement results [81].

imaging and phase shifting, etc. Furthermore, the cloaking feature of metasurfaces can directly change the shape of the wavefront of the reflected wave by counterbalancing the phase difference at different positions distributed along the cloaked surface, without generating any extra phase retardation, in comparison to the bulk materials. Lately, incorporation of the nonlinear phenomena and effects while realizing metasurfaces has been examined on an extensive basis [88]-[91]. Nonlinear metasurfaces are advantageous while providing combined effects of metasurface-based flat optics as well as nonlinear optics; hence, offering a new window for improving the electromagnetic performance and developing new functionalities. Nonlinear metasurfaces can generate large optical nonlinearity and external modulations under the effect of physical excitations. Metasurfaces with the reconfigurability property are most eligible into the current scenario to match the increasing demand in latest optical communication systems for achieving the tunable or switchable characteristics. The properties of the materials can be adjusted electrically, optically, thermally or mechanically. The

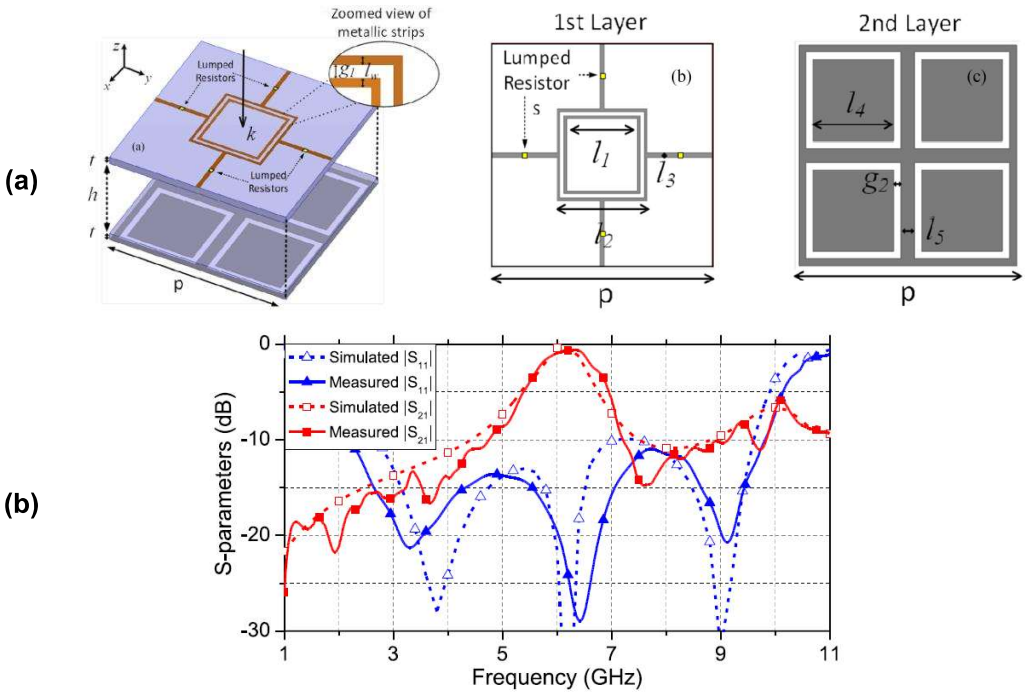

Figure 1.11. Metallic frequency selective structure integrated with lumped components to produce absorption along with a transmission band [82].

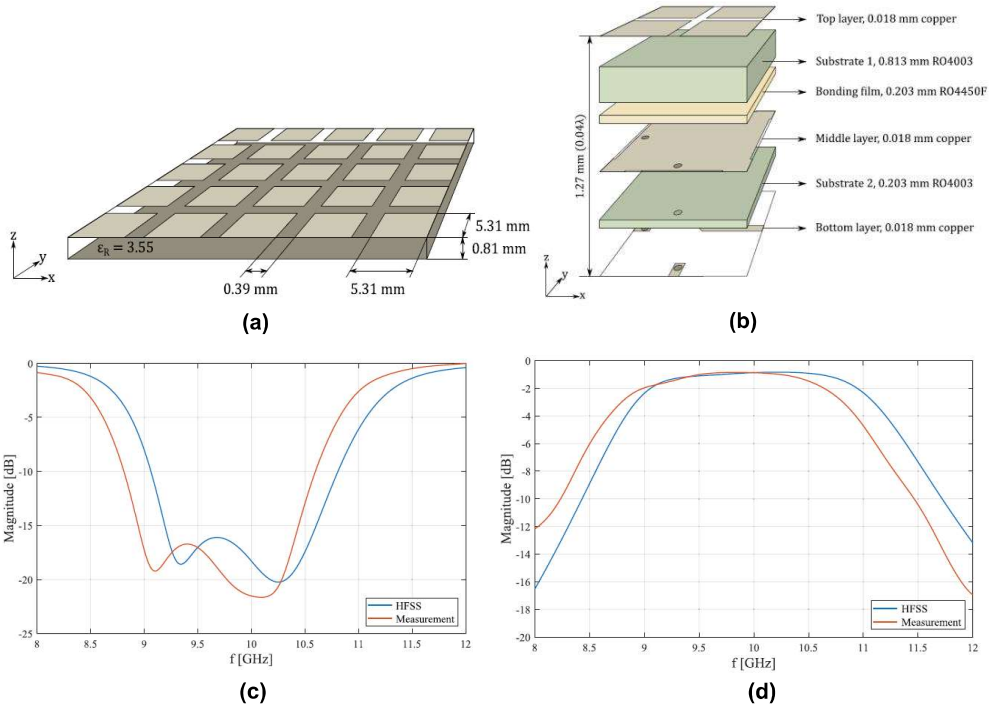

Figure 1.12. (a, b). Multilayer metasurface structure for the cross-polarization manipulation of the electromagnetic wave and (c, d). Comparison of the co- and cross-polarized reflection coefficients extracted from HFSS and measurement [83].

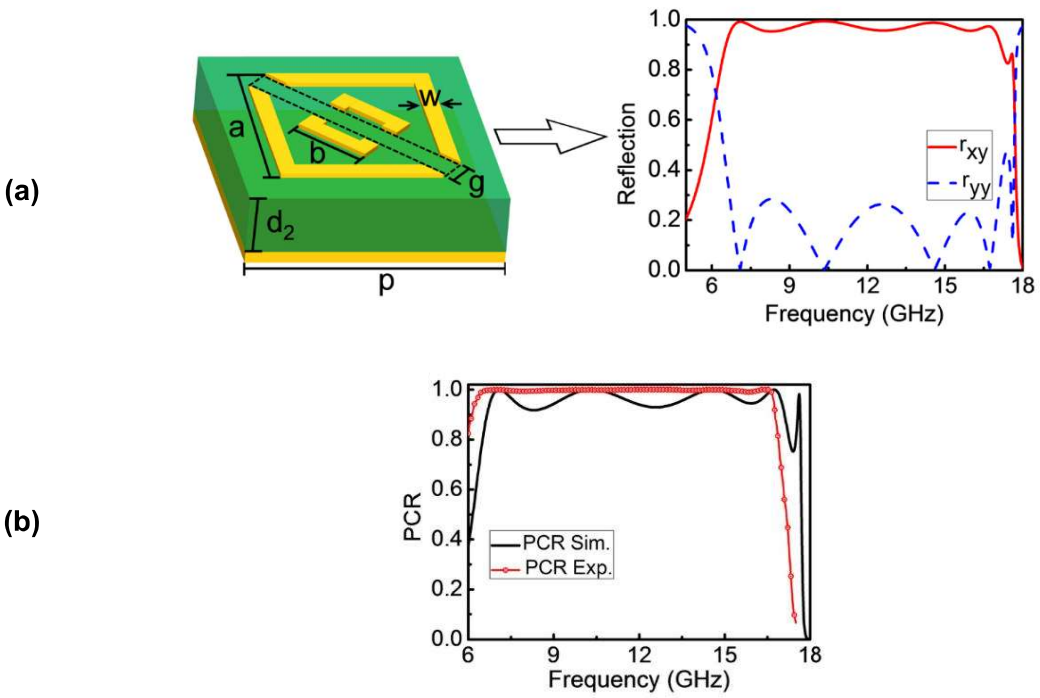

Figure 1.13. (a). Single layer metallic metasurface structure for the cross-polarization conversion of the EM wave and (b). comparison of the simulated and measured co- and cross-polarized reflection coefficients [84].

plasmonic resonances can appear in dielectric and metallic structures within the near-infrared or visible region. The interaction between the EM wave and electrons will be less when the wavelengths increase. As a consequence, the metasurfaces made of dielectric or metal have limited applications in the visible or infrared spectral regions. Additionally, dielectric or metallic meta-atoms distributed in a periodic fashion are fixed geometries; thereby lacking the flexibility to alter their EM responses. Thus, graphene metasurfaces are tempting to the research community because of their ultrathin structure owing to their broadband spectral response and tunable characteristics [92]-[96].

1.4.2 Graphene-based Metasurface: Subsequent Developments

Graphene surface plasmons (GSPs) are excited easily in periodic graphene metasurface-based devices, comprising graphene plasmonic crystals, conductivity gratings, diffraction gratings and corrugated graphene, etc. [93]-[96]. Metallic metasurfaces suffer from unwanted

correlation between amplitude and phase manipulation in optical systems as one meta-atom can produce only one resonance condition. Contrarily, graphene metasurface can offers tunability property in conductivity response under the influence of the external biasing, chemical doping or mechanical stretching of the graphene surface [97]-[100]. Thereafter, the graphene meta-atoms can exhibit multiple resonance conditions from a single structural configuration; which enables them to achieve the complete control of the wavefront. Periodic ribbons structures made of graphene have been deposited in an independent way on top of a dielectric substrate, behaving as tunable terahertz (THz) metasurfaces [101]. Some hybrid configurations of graphene and metal nanostructures have been reported to elevate the spectral performances of the available metallic metasurface-based devices [102]-[103]. Thereafter, singular graphene structures have been implemented to increase the GSPs at the interface of graphene-dielectric metasurface structures for a number of useful applications, *viz.*, absorbers, spatial filters, and cross-polarization converters, etc. [104]-[108]. Ultra-thin compact absorbers have been designed and developed in different spectral regions ranging from microwave to

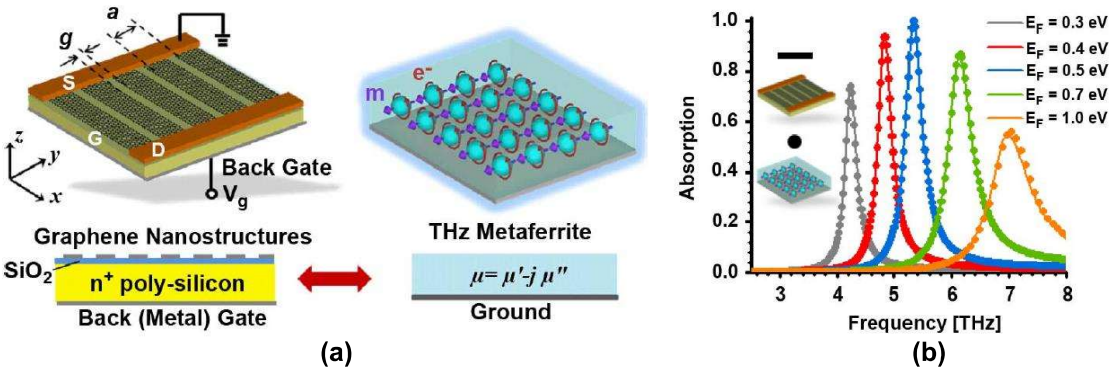

Figure 1.14. (a). Graphene metasurface structure for narrowband electromagnetic wave absorption and (b). absorptivity responses under the variation of the Fermi energy in graphene layer [105].

optical bands [74], [109]. Nevertheless, these structures cannot absorb over a wide frequency band because of high Q of the resonating nature of the metastructure [110]-[111]. Inclusion of lumped elements [112] have been reported to increase the absorption bandwidth, but they are

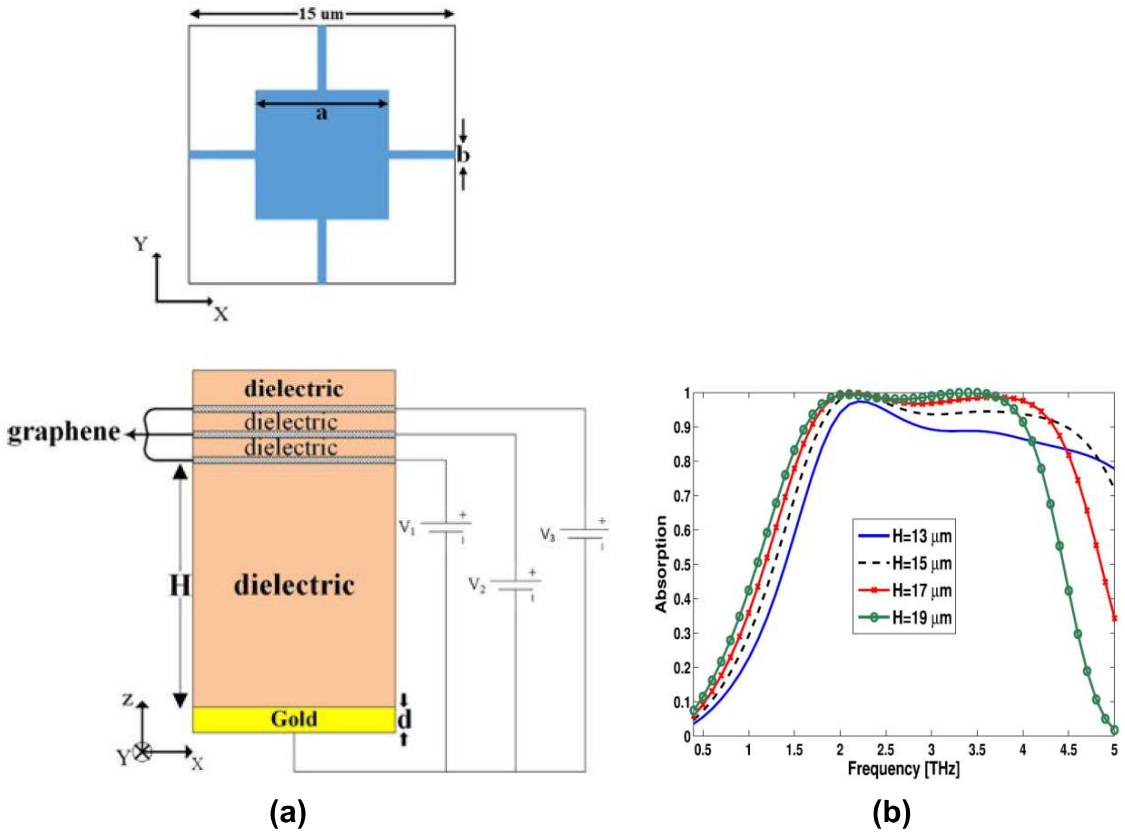

Figure 1.15. (a). Graphene multilayer metasurface structure for wideband electromagnetic wave absorption and (b). absorptivity responses under the variation of the thickness of the substrate [119].

very difficult to realize as well as the structures lose the inherent advantage of using metastructures like compact, ultra-thin and lightweight [113]. Research works on millimeter (mm) wave and higher frequency bands have been explored to study the growth of demand of data to pave the way toward 5G communication system [114]. To allow higher data rates, improved physical security and avoiding EM interference, research works toward optical wireless communication have been potentially increased nowadays [115]. Avoiding EM interference is an important integral part of electromagnetic compatibility. Terahertz gap (0.1–10 THz) can serve as a bridge between mm wave and optical spectrum where naturally available materials cannot be used as they suffer from high loss [116]-[117].

Several literatures presented narrow-band and multi-band absorbers with graphene metasurface [118]-[119]. Narrowband, as well as broadband absorption in the terahertz region, has been

achieved using monolayer graphene and multiple graphene metasurface or multiple dielectric layers or the combination of both which are very unreliable and difficult to fabricate [120]-[125]. Multilayered graphene metasurface with less substrate thickness can be a better solution to the multilayered structures as this arrangement provides wider absorption bandwidth with high reliability, smoother fabrication, etc [126]-[127]. Several theories and explanations are available to validate the working principle of metasurface absorber [124]. Most of the metasurface absorbers have been implemented employing 2-fold symmetry or 4-fold symmetric resistive graphene pattern on the top surface of the substrate so that the overall device can deliver polarization-independent absorption [103]. Control of the electronic

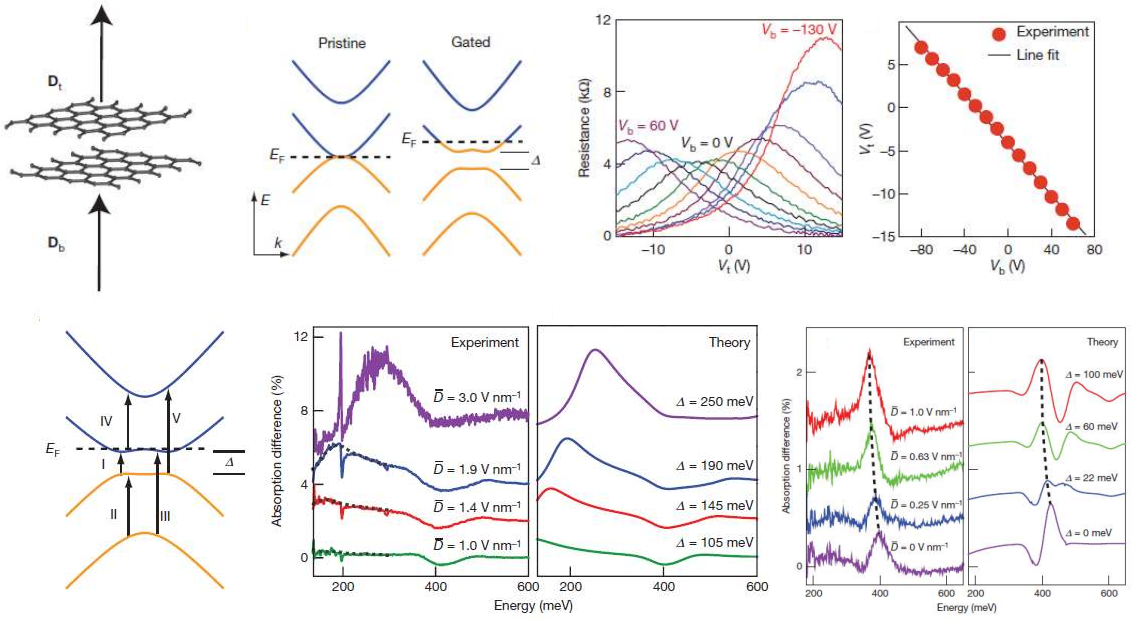

Figure 1.16. Theory and experimental study of un-patterned bi-layer graphene [126].

properties of graphene is highly challenging because of the discrete distribution of graphene energy levels in the periodic boundary conditions [126]. Fermi level of graphene can be adjusted according to the requirements by external doping of impurities or mechanical straining of the graphene layer [128]-[136].

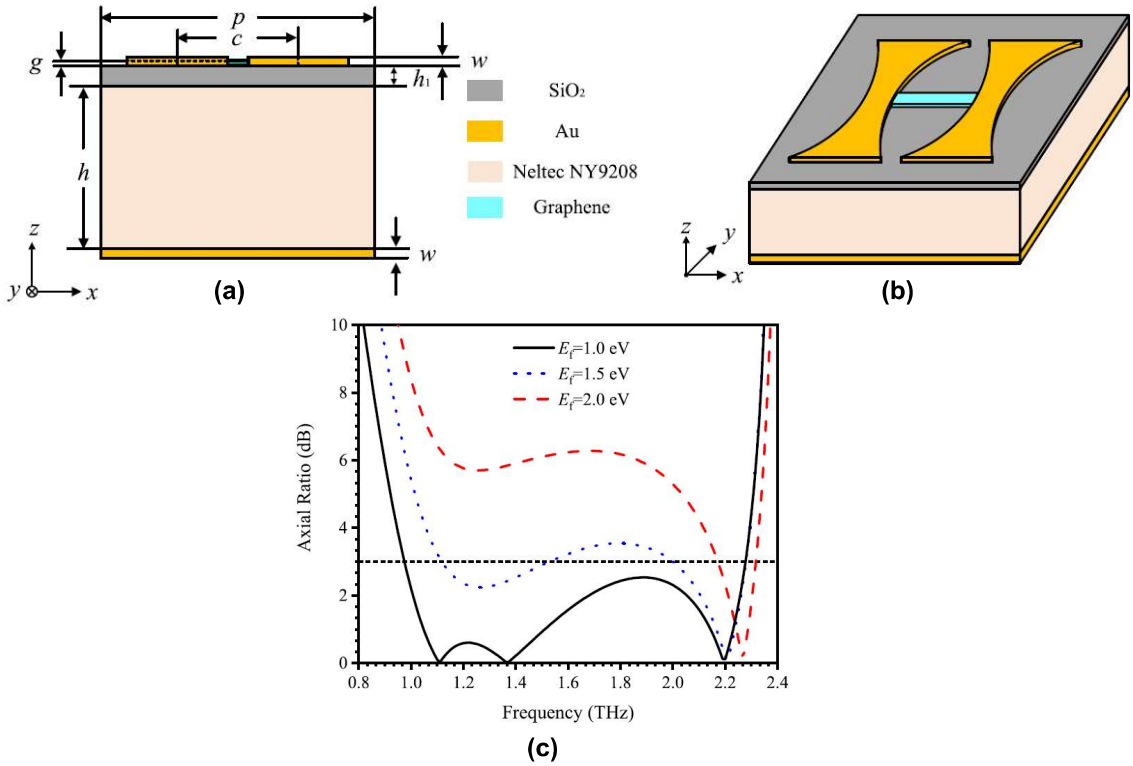

Figure 1.17: (a). Multi-layer metal-graphene hybrid metasurface structure for the reflective circular-polarization conversion of the EM wave and (b). variations of the axial ration response under different Fermi energy values [146].

A new type of devices producing interference-free communication by transmitting the incident EM wave over a chosen band of frequencies beyond the absorption band [137]-[138] have been emerged. These types of devices are called 'rasorbers'. A few metasurface-based three layered rasorbers with metal-dielectric-metal combination were explored in microwave bands [139]-[141], even though their fabrications appear quite challenging. Most of them embody lumped circuit elements resulting in an overall bulky configuration. The subsequent developments aiming to terahertz applications used metal-graphene hybrid metasurfaces [142]-[144] to achieve tunability along with reduction in structural thickness. However, this leads to the limitation of transmission bandwidth.

Three-dimensional chiral metasurfaces have also been proved to be a suitable candidate for the polarization manipulation of the EM wave; however, they have been found difficult to be realized in practice [145]. Later, numerous planar metasurfaces have been introduced as

polarization converter [146]-[148]. Recently, both reflective as well as transmittive type cross-polarization converters have been reported incorporating metasurface designs covering wide spectral domains [149]-[151]. However, generation of circular polarization employing metasurfaces has drawn attention as they find widespread use in antenna applications [152]-[153], polarization converter in the terahertz domain [154], etc. A multi-layer-based metal graphene combined reflective-type structure has been introduced for the circular polarization conversion of the EM wave over a narrow band in lower THz region [155]. But multiple layers will add more conductive and dielectric losses and the physical realization of such devices is challenging. A variety in applications demands both reflective-type as well as transmittive-type polarization converter configurations [156]-[159]. Metasurface-based circular polarization (CP) converters have been preferred owing to their compact configuration and low atmospheric attenuation [156]-[159]. Graphene has been integrated with the metasurface design to offer tunability in the terahertz-gap applications due to its high electrical conductivity, improved optoelectronic properties, remarkable mechanical properties, and durability [160]. A multilayered graphene-based structure and a graphene-metal hybrid metasurface [156], [161] have been explored in lower terahertz region, but their practical implementations seem to be difficult. Metasurface configurations with graphene structures on the substrates [162]-[164] have also been examined for CP conversion of the incident EM wave; nevertheless, the fractional 3-dB axial ratio bandwidth achieved by them is quite narrow.

1.5. Motivation

We have presented our work on graphene metasurface for futuristic THz applications. Metallic meta-atoms carry fixed structures having an insufficient flexibility to control the device. Graphene is a great alternative in 2D configuration metasurface-based designs as it can support surface plasmons as similar as bulk metallic structure. At the same time, graphene is effective

at mid-infrared and lower terahertz frequencies. The purpose of going for the design of graphene metasurfaces is tempting because of its broadband spectral response and tenability.

A few literatures have discussed previously about the need of THz gap applications for modern communication [28-29]. Some of the 2D materials, *viz.*, graphene is very useful for their durability in the THz domain. Dielectric materials like silicon dioxide (SiO_2), zinc oxide (ZnO) have shown a very promising characteristics in the THz and optical domain [107]-[108], [26]-[27]. Over the last decade, research on graphene-based metasurface devices operating in the THz gap has gained attention among the research community globally. Periodic single-layer graphene patterns have been used in the metadevices for various applications in the THz domain [107]-[108]. The tunable surface conductivity of graphene makes it possible to attain versatile characteristics by altering the Fermi level of the graphene [93]-[100].

1.6. Organization of Dissertation

The entire thesis has been organized into six chapters where **Chapter 1** includes the idea about graphene metasurface and their fundamental concept. The concept of two-dimensional (2D) metasurfaces and their applications have been summarized. Thereafter, the introduction of graphene metasurfaces have been incorporated to improve the performance of the device. The basic physics behind the distinctive features of graphene have been discussed. A brief literature survey following some specific literatures has been provided at the last part of this chapter. The motivation and organisation of the thesis have also been stated in this chapter.

Chapter 2 Two types of broadband absorbers have been proposed in this chapter. Broadband absorption of the EM wave is possible because graphene can allocate significantly high plasmonic resonances. The first device has achieved fractional 90% absorption bandwidth. The second prototype reports a higher value of fractional absorption bandwidth of 140.86%. The broadband absorption responses of the above-said two designs have proved the surface

plasmon resonances (SPR) and localized surface plasmon resonances (LSPRs) of the patterned graphene metasurfaces under the exposure of the incident EM wave.

Chapter 3 talks about graphene metasurface-based rasorber having EM wave absorption property as well as transmission property. The configuration of this device includes two sub-wavelength periodic structures on two opposite sides of the substrate. The electromagnetic property of the top graphene metasurface helps to absorb the EM wave efficiently in the lower THz band. The bottom slotted metasurface works as a reflector at some frequencies as well as a filter at other frequencies. Further, all these electromagnetic properties have been validated using inhouse specific circuital approach. Values of all circuit components have been deduced. The EM simulated outputs and the circuit model results are in excellent resemblance.

Chapter 4 includes the design and development of a graphene-based reflective-type slotted metasurface enabling to convert the linearly polarized EM wave into its circularly polarized form. Two elliptical slots arranged perpendicularly have been embedded into one unit cell of the proposed metasurface to manipulate the magnitude and phase of the EM wave. Therefore, under the exposure of the linearly-polarized wave it produces the circularly polarized wave. The proposed metasurface can be easily biased electrically by applying a variable dc voltage between the top and bottom surfaces due to its continuous nature. This device reports a 3 dB axial ratio bandwidth of 2.25 THz within the lower THz region. The tunability property of this device has been verified by producing the polarization ellipses at different ranges of frequencies by externally applied static electric field. Furthermore, the EM simulated results have been compared with the inhouse circuit model approach and they agree well.

This chapter also provides a design illustration of a transmittive-type triple-band linear to circular polarization converter (TTLCPC) within the lower mid-infrared (MIR) region covering the THz gap. The device has a periodic graphene pattern on top surface and the backside of it is covered with a periodically-slotted gold layer. The circular nature of the transmitted wave

has been verified with the calculation of the Stokes' parameters. The design configuration of the TTLCPC has been realized in terms of a circuit schematic to have a clear idea about the device. Further, the circular polarization nature of the transmitted wave at three frequency bands has been verified using an inhouse code by forming polarization ellipses.

Chapter 5 describes the design of a dual-functional metadevice which can be operated for two different applications simultaneously without making any structural deformations. Under the exposure of the EM wave this device can manipulate the wave for absorption as well as cross-polarization conversion under two distinct electric fields. The multi-layered design consists of graphene-metal hybrid combinations to exhibit dual functionality. The device offers more than 70% absorptivity over a bandwidth of 3.40 THz (between 4.25 THz and 7.65 THz) with a 90% absorptivity peak at 6.84 THz under the static electric field of ξ = 8.52 V/nm. The device can also produce a cross-polarization conversion ratio (PCR) more than 90% over a bandwidth of 3.87 THz (between 2.22 THz - 6.09 THz) with near unity PCR peaks at 2.38 THz, 3.80 THz and 5.82 THz, respectively at ξ = 0.44 V/nm. The device is very promising for futuristic applications as it performs dual functionality from a single physical configuration without the integration of lumped elements. The device finds potential applications for THz detection, THz communication, THz imaging, THz sensing, wearable and portable electronic devices, 5G/6G communications and beyond.

Chapter 6 includes the conclusion and future scope of the thesis.